Journal of Marine Science and Technology

Volume 24 | Issue 2 Article 4

EFFECT OF COOLING RATE DURING SOLUTION HEAT TREATMENT ON THE MICROSTRUCTURE AND MECHANICAL PROPERTIES OF SP-700 TITANIUM ALLOYS

Jo-Kuang Nieh
Department of Mechanical Engineering, National Central University, Taoyuan, Taiwan, R.O.C

Chih-Ting Wu
Department of Vehicle Engineering, Army Academy, Taoyuan, Taiwan, R.O.C

Yen-Lin Chen
Institute of Materials Science and Engineering, National Central University, Taoyuan, Taiwan, R.O.C

Chao-Nan Wei
Materials and Electro-Optics Research Division, National Chung-Shan Institute of Science and Technology, Taoyuan, Taiwan, R.O.C.

Sheng-Long Lee
Department of Mechanical Engineering, National Central University,Taoyuan, Taiwan, R.O.C Institute of Materials Science and Engineering, NationalCentral University,Taoyuan, Taiwan, R.O.C.

Recommended Citation

Nieh, Jo-Kuang; Wu, Chih-Ting; Chen, Yen-Lin; Wei, Chao-Nan; and Lee, Sheng-Long (2016) "EFFECT OF COOLING RATE DURING SOLUTION HEAT TREATMENT ON THE MICROSTRUCTURE AND MECHANICAL PROPERTIES OF SP-700 TITANIUM ALLOYS," *Journal of Marine Science and Technology*: Vol. 24: Iss. 2, Article 4.
DOI: 10.6119/JMST-015-0409-1
Available at: https://jmstt.ntou.edu.tw/journal/vol24/iss2/4

EFFECT OF COOLING RATE DURING SOLUTION HEAT TREATMENT ON THE MICROSTRUCTURE AND MECHANICAL PROPERTIES OF SP-700 TITANIUM ALLOYS

Acknowledgements

This work was financially supported by the National ChungShan Institute of Science and Technology. The authors would like to acknowledge National Chung Shan Institute of Science and Technology for providing funding for the study.

Journal of Marine Science and Technology, Vol. 24, No. 2, pp. 99-106 (2016)
DOI: 10.6119/JMST-015-0409-1

EFFECT OF COOLING RATE DURING SOLUTION HEAT TREATMENT ON THE MICROSTRUCTURE AND MECHANICAL PROPERTIES OF SP-700 TITANIUM ALLOYS

Jo-Kuang Nieh[1], Chih-Ting Wu[2], Yen-Lin Chen[3], Chao-Nan Wei[4], and Sheng-Long Lee[1, 3]

Key words: titanium alloy, martensite, heat treatment, mechanical properties.

ABSTRACT

The relationship between the microstructures and the mechanical properties of solution-treated SP-700 titanium alloys, as obtained with different cooling rates, was investigated. The results indicate that the water-quenched alloy contains the primary α (α_p), α"-martensite and residual β (β_r) phases. Aging heat treatment can convert both α"-martensite and the β_r phases to the fine-grained α + β equilibrium phases, resulting in a significant increase in tensile strength and hardness. Both the air-cooled and furnace-cooled alloys consist of the α_p, α and β phases. The air-cooled alloy containing the fine-grained α phase has relatively higher hardness. Aging heat treatment causes only a slight enhancement in tensile properties because it cannot convert the phases in both alloys. Stress-induced martensitic phase transformation occurs in the water-quenched alloy under applied stress, after which the alloy exhibits higher tensile strength, higher ductility, and lower yield strength.

I. INTRODUCTION

SP-700, a β-rich α + β titanium alloy, has excellent hot/cold formability, superplasticity, and mechanical properties (Ishikawa et al., 1992; Ouchi, 1993). The appropriate heat treatment and cooling methods can produce fine grains (2 to 3 μm) and increase the strength of the titanium alloy to as much as 1200 MPa. After annealing heat treatment, the titanium alloy can be cold formed (Ouchi, 1993; Brewer et al., 1998; Gunawarman et al., 2001). Due to its lower β-transus temperature (~900°C), this process can extend the life of a die. In addition to applications in aerospace, SP-700 titanium alloy is also widely employed in automobiles, sporting goods, golf club faces, and hand tools (Ogawa et al., 1996).

Regions of the α + β two-phase in SP-700 titanium alloy preferentially precipitates the primary α (α_p) and β phases during solution heat treatments. The following quenching lowers the temperature rapidly below Martensite start temperature (M_s), resulting in a martensitic transition and the presence of α' or α"-martensite. Because Martensite finish temperature (M_f) is below room temperature (Brooks, 1982), not all of the β phase can transform into α' or α"-martensite. The remaining β phase retains its original microstructure at room temperature and is known as the residual β phase (β_r). After aging heat treatment, both martensite and the β_r phases convert into the equilibrium α + β phases (Brooks, 1982; Polmear, 1995). If the alloy is slowly cooled to room temperature after solution heat treatment, the α phase will precipitate within the β phase matrix. This phenomenon is observed because solute atoms have sufficient time to diffuse at a lower cooling rate. There is no apparent phase transformation and a near-equilibrium composition in both the α and β phases can be obtained (Brooks, 1982; Polmear, 1995).

Because the strength of the α phase is greater than that of the β phase at room temperature, the strength of the alloy can be enhanced by increasing the portion of the α phase in the alloy. In this way, the quantity and morphology of the α phase governs the strength of titanium alloys (Kao et al., 2005). Thus, SP-700 titanium alloys can be strengthened through proper precipitation heat treatment (Ouchi, 1993). The temperature of solution heat treatment directly dominates the quantity and morphology of both the α and β phases and, as a

Paper submitted 12/31/14; revised 04/04/15; accepted 04/09/15. Author for correspondence: Sheng-Long Lee (e-mail: shenglon@cc.ncu.edu.tw).
[1] *Department of Mechanical Engineering, National Central University, Taoyuan, Taiwan, R.O.C.*
[2] *Department of Vehicle Engineering, Army Academy, Taoyuan, Taiwan, R.O.C.*
[3] *Institute of Materials Science and Engineering, National Central University, Taoyuan, Taiwan, R.O.C.*
[4] *Materials and Electro-Optics Research Division, National Chung-Shan Institute of Science and Technology, Taoyuan, Taiwan, R.O.C.*

Table 1. Chemical composition of experimental alloy.

Alloy element	Al	V	Mo	Fe	C	O	N	H	Ti
Content (wt.%)	4.41	2.89	1.89	1.85	0.01	0.14	0.01	N.D.	Rem.

N.D.: not detectable; Rem.: remainder

result, affects the mechanical properties of the alloy. Solution heat treatment at higher temperatures can decrease the size of α_p grains, which can lead to an increase in tensile strength and a decrease in ductility (Zhang et al., 2010). Solution heat treatment above 800°C of the $\alpha + \beta$ two-phase regions with subsequent water quenching and tensile stress can induce the formation of martensite in SP-700 titanium alloy at room temperature. This stress-induced martensitic transformation can produce a hardening effect that is comparable to work-hardening. Increasing the solution-heat-treatment temperature, increases the stress-induced formation rate of martensite, and increases the maximum tensile strength that can be obtained (Ouchi et al., 1999).

Solution-heat-treatment temperature plays an important role in age-strengthening (Ouchi et al., 1999; Zhang et al., 2010). At higher temperatures, the martensite and the β_r phase are more prone to form after water quenching. After aging heat treatment, the alloys subjected to higher solution-heat-treatment temperatures can form the more-fine-grained equilibrium $\alpha + \beta$ phases, which leads to a significant enhancement of the strength of the alloy.

Solution treated SP-700 titanium alloys undergo a martensitic phase transformation during the cooling process. Although different cooling rates can change the microstructure and mechanical properties of the alloy, exactly how the cooling rate affects the mechanical properties of solution-treated SP-700 titanium alloy remains unclear. Water quenching, air cooling, and furnace cooling are employed in the present study to investigate the effect of the cooling rate of the treatment solution on the microstructure and mechanical properties of SP-700 titanium alloys.

II. EXPERIMENTAL PROCEDURES

Commercial SP-700 titanium alloy (Ti-4.5Al-3V-2Mo-2Fe) cylindrical rods of 45 mm diameter were used in the present study. The nominal chemical composition of the alloy is given in Table 1. The experimental alloy was annealed at 720°C for two hours, then rectangular specimens with the size of 50 mm long × 7 mm wide × 7 mm thick were cut from the annealed cylindrical rods for solution heat treatment in a furnace with a protective atmosphere at 850°C for one hour, and subsequently cooled by water quenching, air cooling, or furnace cooling with cooling rates were around 200°Cs^{-1}, 10°Cs^{-1}, and 0.1°Cs^{-1} before artificial aging at 500°C for one hour. Chemical etching according to ASTM E407 in the Kroll's reagent (2% HF+ 6% HNO_3+ 92% H_2O) was applied after grinding and polishing. The microstructure of the experimental alloy was observed by optical microscopy (OM) and scanning electron microscopy (SEM) employing an image analyzer. X-ray powder diffraction (D8A, Bruker) was adopted to determine the phases in the alloy and an electron probe micro analyzer (JXA-8800M) was used for a compositional analysis of the precipitate phases.

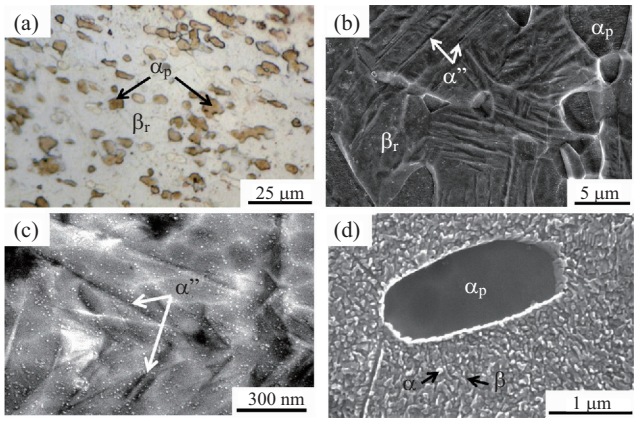

Fig. 1. Micrograph of water-quenched alloy (a) OM, (b) SEM, (c) High magnification SEM, (d) SEM after aging.

The characterization of the precipitation in the experimental alloys was examined using a differential scanning calorimeter (DSC) (DSC22C-SSC5100). The DSC runs were made at a heating rate of 10°C/min from 25 to 600°C. The hardness was determined using a Vickers hardness tester. The loading weight and loading time were 1 kgw and 10 s, respectively. Round tensile bars with a diameter of 6.25 mm were tested according to the standard testing method, ASTM E8-04 (ASTM E8-04, 2004), with tensile strain rate of 0.2/min and gauge length of 25.4 mm.

III. RESULTS AND DISCUSSION

1. Microstructure

1) Water-Quenched Alloy

Fig. 1(a) shows that block-like α_p phases (Ti-5.7Al-1.8V-0.2Mo-0.1Fe) with the average size of 3.4 μm and volume fraction of 21.89% are distributed within the β_r matrix (Ti-4Al-4.1V-2.2Mo-2.2Fe) of the water-quenched alloy. The SEM micrograph further indicates that plate-like α"-martensite is also distributed in the β_r phase, as shown in Fig. 1(b). Fig. 1(c), a higher magnification of image in Fig. 1(b), also indicates that these extremely small interwoven α"-martensite plates are distributed throughout the β_r matrix. The SP-700 titanium alloy contains both the α_p and β phases at approximately 850°C in the two-phase region (Attallah et al., 2009).

During water quenching, the atoms in the solid phase are less prone to diffuse. This property leads to a partial martensitic transformation of the β phase to fine-grained α”-martensite (Gunawarman et al., 2001; Lyasotskaya and Knyazeva, 2008). Because the M_f temperature of SP-700 titanium alloy is far lower than room temperature (Brooks, 1982), the martensitic transformation is incomplete. The remaining β phase that cannot transform into fine-grained α”-martensite is known as the residual β phase (β_r). The final microstructure of the water-quenched alloy consists of the α_p, α”-martensite, and the β_r phases.

However, aging heat treatment of the water-quenched alloy transforms α”-martensite and the β_r phases into the equilibrium α + β phases. This result is consistent with the image in Fig. 1(d), which shows that the water-quenched alloy contains the α and β phases after aging heat treatment. Both α”-martensite and the β_r phases can transform into the equilibrium α + β phase during aging heat treatment. This property is observed because α”-martensite contains a β-stabilizing element that makes it a supersaturated solid solution. The precipitation of the β phase can reduce the concentration of the β-stabilizing element in the α”-martensite, transforming the α”-martensite into the equilibrium α phase during aging heat treatment (Brooks, 1982). After aging heat treatment, the β phase can be determined within the α phase. In addition to the α”-martensite transformation, the β_r phase can also be transformed into the equilibrium α + β phases during aging heat treatment. β_r is a residual phase of high temperatures and the concentration of the β-stabilizing element in the β_r phase is lower than the equilibrium concentration at room temperature. Thus, the aging heat treatment can produce a precipitation of the α phase from the β_r phases that leads to an increase in the concentration of the β-stabilizing element in the β_r matrix. The increase in the concentration of the β-stabilizing element can convert the β_r phase to the equilibrium β phase (Gunawarman et al., 2001).

The x-ray diffraction (XRD) analysis confirms that the microstructure of the water-quenched alloy consists of the α_p, α”-martensite, and the β_r phases, as shown in Fig. 2(a). After aging heat treatment, both the β_r phase and α”-martensite transform into the α + β phases. This transformation was demonstrated by the absence of the diffraction peak of the α”-martensite phase in the XRD pattern and by the presence of only α- and β-phase signals. In addition, the peak corresponding to the β phase—approximately 2θ = 39°—cannot be found after aging heat treatment because the radii of the solute atoms (Al: 118, V: 122, Mo: 130, Fe: 117 pm) are smaller than the radius of the titanium atom (132 pm). These solute atoms in SP-700 titanium alloy are considered to be substitutional. When the concentration of solute atoms increases, the lattice constant becomes smaller and the XRD angle increases, which causes the peaks in the XRD pattern shift to the right. From the simulation phase diagram of the titanium alloy (Attallah et al., 2009), it is reasonable to deduce that the concentration of solute atoms in the β_r phase of the water-quenched alloy is

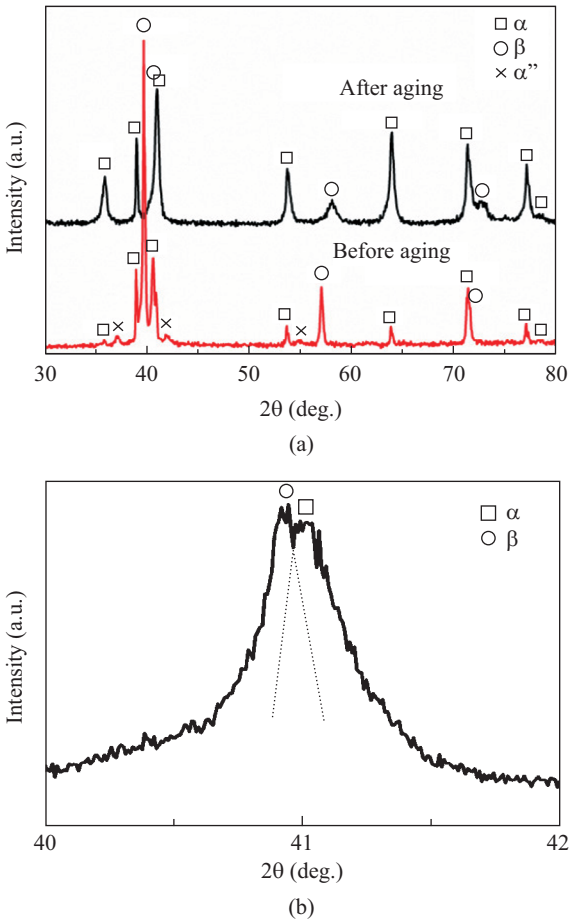

Fig. 2. X-ray diffraction pattern of water-quenched alloy (a) before and after aging, and (b) slow scan of 0.01°/s and high resolution angle 2θ = 40°~42°.

lower than that of the β equilibrium phase. During aging heat treatment, the α phase precipitates from the β_r phase and leads to a transformation of the β_r phase to the β phase. Because β_r phase with a low concentration of solute atoms converts to β phase with a high concentration of solute atoms, the XRD peak of the β phase shifts to the right, close to the α phase peak (2θ = 41°). Fig. 2(b) shows results of the XRD analysis conducted at slower scanning speeds and at high angular resolution. Two close diffraction peaks can be observed. Because the diffraction peaks of the α and β phases are close, they cannot be distinguished at faster scanning speeds, shown in Fig. 2(a). Similarly, aging heat treatment increases the concentration of solute atoms in the α_p phase, bringing it close to the concentration of solute atoms in the α phase, which converts from the α_p phase or α”-martensite. This causes the diffraction peaks of the α phase to shift slightly to the right. The diffraction peak of the β phase shifts even more to right than that of the α phase, indicating that variation in the concentration of solute atoms of the β phase exceeds that of the α phase.

The water-quenched alloy consists of a large amount of the

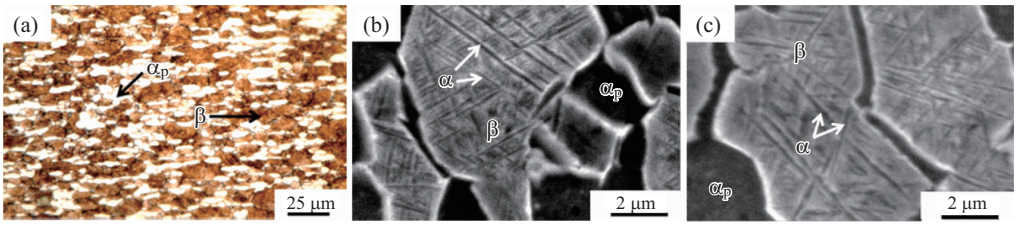

Fig. 3. Microstructures of the alloy solution treated at 850°C and air cooling (a) OM, (b) SEM, and (c) SEM plus aging.

β_r phase and a relatively small amount of α"-martensite and α_p phases. After aging treatment, both α"-martensite and the β_r phases transform into the α + β equilibrium phases, resulting in an increase in the amount of the α phase and a decrease in the amount of the β phase. This phenomenon can be further verified with the XRD pattern. As shown in Fig. 2(a), the intensity of the peaks corresponding to the α phase increases after aging heat treatment, indicating an increase in the amount of the α phase. In contrast, the intensity of the peaks corresponding to the β phase decreases after aging heat treatment, which indicates a decrease in the amount of the β phase. Therefore, phase transformation during aging heat treatment is consistent with the analysis of the XRD pattern.

2) Air-Cooled Alloy

Fig. 3 indicates the absence of α"-martensite in the air-cooled alloy. This absence is observed because the cooling rate of air-cooling is much lower than the cooling rate of water quenching. The air-cooling is relatively close to equilibrium cooling, and therefore martensitic transformation does not occur during air-cooling process. Air cooling can cause a precipitation of the α phase within the β matrix. Thus, the microstructure of the air-cooled alloy is composed of the α_p, α, and β phases. The α_p (Ti-5.6Al-1.8V-0.3Mo-0.1Fe) and β phases (Ti-2.9Al-4.7V-2.7Mo-3.7Fe) can be observed in Fig. 3(a). Compared to the water-quenched alloy in Fig. 1(a), the average size of 3.9 μm and volume fraction of 30.43% of α_p phase in air-cooled alloy are larger than those of water-quenched alloy. Fig. 3(b), the magnified region of the β phase, shows a small amount of α precipitates within the β matrix. Because there are many α/β phase interfaces within the β phase, the surface is not smooth after etching. This rough surface scatters light, resulting in the β phase appearing darker under optical microscopy.

Fig. 3(c) shows the microstructure of the air-cooled alloy after aging heat treatment. As the solute atoms diffuse during the air-cooling process, sufficient concentrations of β-stabilizing elements within the β phase can be obtained at room temperature. Compared to the water-quenched alloys, the amount of β-stabilizing element in the air-cooled alloy is closer to that of the equilibrium β phase (Brooks, 1982). Aging heat treatment does not cause a phase transition, therefore, the air-cooled alloy contains the α_p, α, and β phases before and after aging heat treatment. Fig. 4 shows the presence of both the α and β phases in the air-cooled alloy before and after

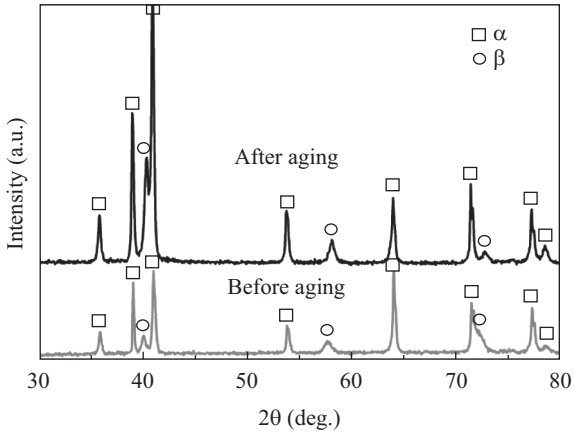

Fig. 4. X-ray diffraction pattern of air-cooled alloy before and after aging heat treatment.

aging heat treatment. The aging process does not cause a shift in XRD peak of the α phase, but causes the peak of the β phase shift toward the right. From the simulation phase diagram of the titanium alloy (Attallah et al., 2009), the gradient of the α phase solidus is greater than that of the β phase, which means the variation in equilibrium composition of the α phase from high to low temperatures is small compared to that of the β phase. During air cooling, the α phase easily becomes the equilibrium phase. Thus, the aging heat treatment has a negligible effect on the composition of the α phase. As a result, the peak of the α phase has the same location before and after aging heat treatment, as shown in Fig. 4. In contrast, the air-cooled alloy still contains a small quantity of the β_r phase, which leads to a change in composition after aging heat treatment, resulting in a slight shift of the β peak. The intensity of the α and β peaks are consistent before and after aging heat treatment, which indicates that there is no obvious change in the concentrations of the two phases within the alloy.

3) Furnace-Cooled Alloy

Due to its low cooling rate, no martensite forms during the furnace cooling process. The low cooling rate leads to the precipitation of the α phase from the β phase and the grain coarsening of the α phase (Gunawarman et al., 2001). The microstructure of the furnace-cooled alloy is similar to the equilibrium condition. In other words, the furnace-cooled alloy contains the α_p, coarse-grained α, and β phases—shown in Fig. 5(a). The average size of 5.2 μm and volume fraction

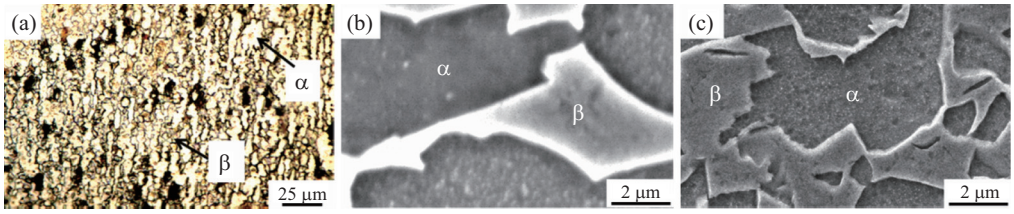

Fig. 5. Microstructures of the alloy solution treated at 850°C and furnace cooling (a) OM, (b) SEM, and (c) SEM plus aging.

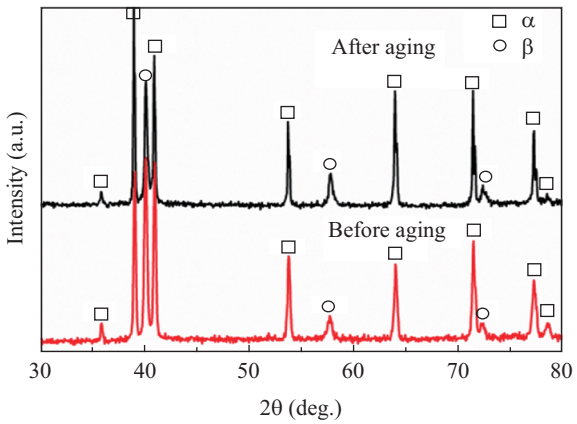

Fig. 6. X-ray diffraction pattern of furnace-cooled alloy before and after aging heat treatment.

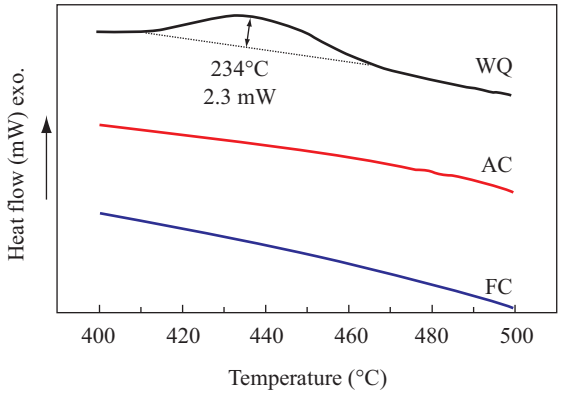

Fig. 7. DSC traces of experimental alloys.

of 37.63% of α phase in the furnace-cooled alloy are slightly larger than those in the air-cooled and water-quenched alloys. This property can be observed and verified by comparing Figs. 5(a), 3(a) and 1(a). Fig. 5(b), a high magnification SEM image, shows the absence of the α phase precipitated within the β phases, which suggests that the α and α_p phases combine during furnace cooling, resulting in the large α_p phase can be observed under an optical microscope. In Fig. 5(a), several black regions can be observed that are similar to the β phases in the air-cooled alloy. The β phases contain a small amount of precipitated α phase, resulting in dark regions under an optical microscope.

Fig. 5(c) shows the microstructure of the furnace-cooled alloy after aging heat treatment. Because the cooling rate of furnace cooling is slower than that of air cooling, the furnace cooling is closer to equilibrium cooling, allowing solute atoms to diffuse freely. Thus, the β phase contains sufficient β-stabilizing elements in the furnace-cooled alloy at room temperature to become equilibrium β phase. Even after aging heat treatment, the furnace-cooled alloy has the same microstructure as it did before. The XRD pattern of the furnace-cooled alloy, shown in Fig. 6, reveals that both the α and β phases are present, and there is no obvious shift in the locations of the peaks before and after aging heat treatment. This indicates that the concentration of solute atoms in the α and β phases does not change over the course of aging heat treatment. The intensity of the diffraction peaks remains consistent after the aging process, which suggests that the amount of the α and β phases remains constant.

2. Calorimetric Studies

Aging heat treatment can cause α”-martensite and β_r phases to transform into equilibrium α + β phases. To investigate this phenomenon, a differential scanning calorimetry (DSC) is performed to obtain the thermodynamic parameters associated with heat-induced phase transformation. Unfortunately, the transformation of the β_r phase cannot be easily measured by DSC because of its extremely low precipitation kinetics (Sha and Guo, 1999). Only the exothermal peak of the transformation of α”-martensite to the equilibrium α + β phases could be measured in the present study. Fig. 7 shows the DSC traces of the three experimental alloys from 25°C to 600°C. It is clear that only the water-quenched alloy has an exothermic peak during 410°C to 460°C. In the contrast, an exothermic peak cannot be found in the DSC traces of both the air-cooled and the furnace-cooled alloys. This result indicates that a phase transformation of α”-martensite to the equilibrium α + β phases occurs only in the water-quenched alloy and does not occur in the air-cooled and furnace-cooled alloys.

3. Mechanical Characteristics

1) Hardness Properties

The strength ranking of the precipitates in the experimental alloy is α > α” > β (Kao et al., 2005). That is, the strength of the alloy depends mainly on the amount of α phase in the alloy. As discussed in section 1.1, the water-quenched alloy contains the α_p phase, α”-martensite, and the β_r phases. The air-cooled alloy consists of the α_p, fine-grained α, and β phases and the furnace-cooled alloy consists of the α_p, coarse-grained α, and β phases. Because both air-cooled and furnace-cooled alloys

Table 2. Mechanical properties of experimental alloys before and after aging.

Mechanical properties / Alloy	Hardness (HV)	0.2%YS (MPa)	UTS (MPa)	El. (%)
Water-Quenched (P_{WQ})	279 (7.4)	540 (5.3)	1118 (8.4)	18.2 (0.2)
Air-cooled (P_{AC})	355 (5.6)	990 (6.1)	1143 (9.2)	14.6 (0.3)
Furnace-cooled (P_{FC})	326 (9.3)	910 (6.9)	990 (6.5)	16.7 (0.3)
Water-Quenched/aged (P_{WQa})	470 (6.6)	1273 (8.2)	1466 (10.1)	4.3 (0.1)
Air-cooled/aged (P_{ACa})	391 (9.6)	1187 (7.0)	1316 (9.9)	12.2 (0.3)
Furnace-cooled/aged (P_{FCa})	344 (4.5)	943 (6.6)	1067 (8.9)	15.6 (0.1)

Standard deviations are listed in parentheses.

P_{WQ}: Water Quenching; P_{AC}: Air-cooling; P_{FC}: Furnace-cooling; P_{WQa}: Aged after Water Quenching; P_{ACa}: Aged after Air-cooling; P_{FCa}: Aged after Furnace-cooling.

contain α precipitates, they have higher hardness than that of the water-quenched alloy, as shown in Table 2. Furthermore, the hardness of the air-cooled alloy is greater than that of the furnace-cooled alloy, mainly because the former has relatively fine-grained α precipitates.

Table 2 also shows the mechanical properties of the experimental alloys after aging heat treatment. During the aging heat treatment, both α”-martensite and the β_r phases transform into the fine-grained equilibrium α + β phases. In addition to the precipitation strengthening of the α phase, these fine-grained equilibrium α + β phases can enhance hardness because of the grain refinement strengthening (Brooks, 1982; Polmear, 1995). Table 2 shows that aging heat treatment causes an increase in the hardness of the experimental alloys, which is consistent with the microstructural examination. The variation in the hardness of the water-quenched alloy is more obvious than that of the other alloys. This is mainly because it consists of both α”-martensite and the β_r phases, producing the largest number of the fine-grained α + β equilibrium phases during aging heat treatment. In contrast, the absence of α”-martensite and the presence of a relatively small amount of the β_r phase in the air- and furnace-cooled alloys only cause a slight increase in hardness after aging heat treatment. In summary, the hardness of the water-quenched alloy enhanced more by the aging heat treatment than the air- and furnace-cooled alloys.

2) Tensile Properties

In general, materials with greater hardness or tensile strength have lower plastic deformation capacity, which can cause poor ductility and toughness. In the present study, the water-quenched alloy has relatively low hardness, high ductility, and excellent tensile strength, as shown in Table 2. This can be explained by the stress-strain curves, as presented in Fig. 8. The water-quenched alloy undergoes significant work hardening as a result of stress-induced martensitic phase transformation during tensile testing. Because solute atoms hardly diffuse during water-quenching, the β phase partially undergoes martensitic transformation to α”-martensite and the

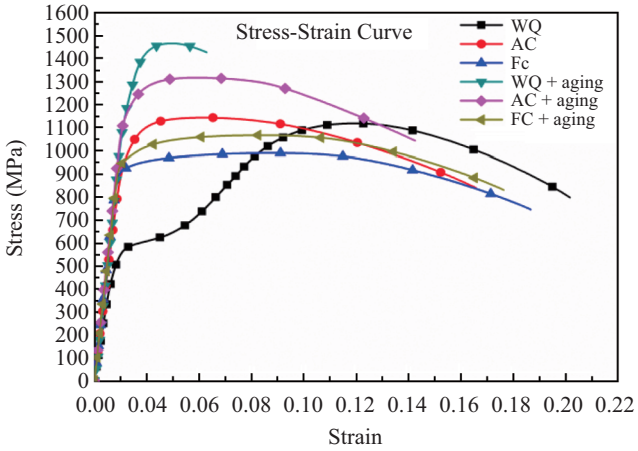

Fig. 8. Stress-strain curves of experimental alloys before and after aging.

remaining β phase becomes β_r phase that retains the microstructure of high temperatures at room temperature. When tensile stress is applied to the alloy, martensitic transformation of the β_r phase to α” -martensite occurs and the crystal structure becomes more stable. This phenomenon is well known as stress-induced martensitic transformation (Ouchi et al., 1999; Ohmori et al., 2001). However, high shear-strain easily causes martensitic transformation of the β_r phase into the α phase (Reed-Hill and Abbaschian, 1994). Fig. 9 shows the XRD pattern of the water-quenched alloy after cold working. The absence of the diffraction peak of the β phase indicates that the β_r phase transforms to α phase and α”-martensite as a result of stress-induced martensitic transformation during cold working. Because the strength of the α phase and α”-martensite is higher than that of the β phase (Kao et al., 2005), the tensile testing causes stress-induced martensitic transformation of the β_r phase to the α phase and leads to an increase in tensile strength of the alloy. Thus, the water-quenched alloy exhibits both high tensile strength and ductility. In contrast, Fig. 8 reveals that martensitic transformation does not occur in either the air-cooled or the furnace-cooled alloys. The tensile strength depends mainly on the quantities of the

Table 3. Relative change in mechanical properties before and after aging.

Mechanical Properties	ΔHardness	Δ0.2%YS	ΔUTS	ΔEl.
Water Quenching $(\frac{P_{WQa} - P_{WQ}}{P_{WQ}}) \times 100\%$	69%	135%	31%	-76%
Air-cooling $(\frac{P_{ACa} - P_{AC}}{P_{AC}}) \times 100\%$	10%	20%	15%	-16%
Furnace-cooling $(\frac{P_{FCa} - P_{FC}}{P_{FC}}) \times 100\%$	6%	4%	8%	-7%

P_{WQ}: Water Quenching; P_{AC}: Air-cooling; P_{FC}: Furnace-cooling; P_{WQa}: Aged after Water Quenching; P_{ACa}: Aged after Air-cooling; P_{FCa}: Aged after Furnace-cooling.

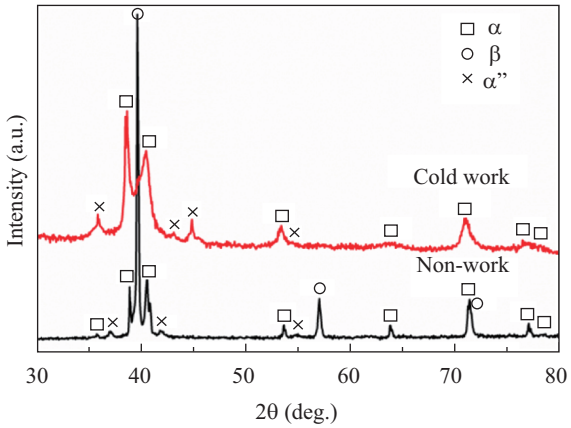

Fig. 9. XRD pattern of water-quenched alloy before and after cold working.

α phases and their grain size in both alloys. The tensile strength of the furnace-cooled alloy is inferior to that of the air-cooled alloy because the former has coarser-grained α phase than the latter. In addition, the furnace-cooled alloy with lower tensile strength has better ductility than that of the air-cooled alloy, as shown in Table 2. After aging heat treatment, the tensile strengths of all the experimental alloys increase, as presented in Table 3. The percentage change in tensile properties of the water-quenched alloy is much higher than the air-cooled and the furnace-cooled alloys. This is because of the precipitation strengthening effect of the α + β phases in the water-quenched alloy during aging heat treatment. In contrast, both air- and furnace-cooled alloys do not contain α"-martensite and therefore cannot precipitate the α + β phases. Thus, the tensile properties of both alloys only change slightly after aging heat treatment.

IV. CONCLUSIONS

The effect of the cooling rate during solution heat treatment on the microstructure and mechanical properties of SP-700 titanium alloys has been investigated. The results are summarized as follows:

1. Water-quenched alloy contains the α_p phase, α"-martensite and the β_r phases. Aging heat treatment can convert both α"-martensite and the β_r phases to the fine-grained α + β equilibrium phases, resulting in a significant increase in tensile strength and hardness.
2. Both the air-cooled and the furnace-cooled alloys contain the α_p, α and β phases. The air-cooled alloy contains finer-grained α phase and has relatively greater hardness. Aging heat treatment causes only a slight enhancement in tensile properties because it cannot convert the phases in the alloys.
3. Stress-induced martensitic phase transformation occurs in water-quenched alloy under applied stress and causes the alloy to exhibit higher tensile strength, higher ductility, and lower yield strength.

ACKNOWLEDGMENTS

This work was financially supported by the National Chung-Shan Institute of Science and Technology. The authors would like to acknowledge National Chung Shan Institute of Science and Technology for providing funding for the study.

REFERENCES

ASTM E8-04 (2004). Standard Test Methods for Tension Testing of Metallic Materials, ASTM International, West Conshohocken, PA.

Attallah, M. M., S. Zabeen, R. J. Cernik and M. Preuss (2009). Comparative determination of the α/β phase fraction in α + β-titanium alloys using x-ray diffraction and electron microscopy. Materials Characterization 60, 1248-1256.

Brewer, W. D., R. K. Bird and T. A. Wallace (1998). Titanium alloys and processing for high speed aircraft. Materials Science and Engineering A 243, 299-304.

Brooks, C. R. (1982). Heat Treatment, Structure and Properties of Nonferrous Alloys. ASM, Metals Park, Ohio.

Gunawarman, A., M. Niinomi, K. Fukunaga, D. Eylon, S. Fujishiro and C. Ouchi (2001). Fracture characteristics and microstructural factors in single and duplex annealed Ti-4.5Al-3V-2Mo-2Fe. Materials Science and Engineering A 308, 216-224.

Ishikawa, M., O. Kuboyama, M. Niikura, C. Ouchi (1992). Microstructure and mechanical properties relationship of β-rich α-β titanium alloy; SP-700. Proceeding of the seventh World Titanium Conference, San Diego,

California, USA. 141-148.

Kao, Y. L., G. C. Tu, C. A. Huang and T. T. Liu (2005). A Study on the hardness variation of α- and β-pure titanium with different grain sizes. Materials Science and Engineering A 398, 93-98.

Lyasotskaya, V. S. and S. I. Knyazeva (2008). Metastable phases in titanium alloys and conditions of their formation. Metal Science and Heat Treatment 50, 373-377.

Ogawa, A., M. Niikura, C. Ouchi, K. Minikawa and M. Yamada (1996). Development and applications of titanium alloy SP-700 with high formability. Journal of Testing and Evaluation 24, 100-109.

Ohmori, Y., T. Ogo, K. Nakai and S. Kobayashi (2001) Effects of ω-phase precipitation on β→α, α" transformations in a metastable β titanium alloy. Materials Science and Engineering A 312, 182-188.

Ouchi, C. (1993). Development and application of new titanium alloy SP-700. Proceeding of the First International Symposium on Metallurgy and Technology of Practical Titanium Alloys, Chiba, Japan. 37-44.

Ouchi, C., H. Fukai and K. Hasegawa (1999). Microstructural characteristics and unique properties obtained by solution treating or aging in β-rich α + β titanium alloy. Materials Science and Engineering A 263, 132-136.

Polmear, I. J. (1995). Light Alloys: Metallurgy of the Light Metals. Edward Arnold, London.

Reed-Hill, R. E. and R. Abbaschian (1994). Physical Metallurgy Principles, PWS, Boston.

Sha, W. and Z. L. Guo (1999). Phase evolution of Ti–6Al–4V during continuous heating. Journal of Alloys and Compounds 290, L3-L7.

Zhang, G. and F. S. Zhang (2010). Effect of heat treatment process on structures and properties of SP-700 titanium alloy. The Chinese Journal of Nonferrous Metals 20, 664-669.